Revista Brasileira de Geofísica
RBGf
Brazilian Journal of Geophysics

Revista Brasileira de Geofísica (2011) 29(1): 43-56

ISSN 0102-261X
www.scielo.br/rbg

A REMOTE SENSING DERIVED UPPER OCEAN HEAT CONTENT DATASET FOR THE EQUATORIAL ATLANTIC: COMPARISON WITH PIRATA PROJECT DATA

Wilton Zumpichiatti Arruda[1,3] and Carlos Alessandre Domingos Lentini[2,3]

Recebido em 3 maio, 2010 / Aceito em 21 janeiro, 2011
Received on May 3, 2010 / Accepted on January 21, 2011

ABSTRACT. In this work, nine years (1998-2006) of Sea Level Anomalies (SLA) from multimission altimeter data distributed by Archiving Validation and Interpretation of Satellite Data in Oceanography (AVISO) were combined with Sea Surface Temperature (SST) data from the TRMM Microwave Imager and climatological subsurface data from World Ocean Atlas 2001 (WOA01) through a reduced gravity model, as well as a statistical model, to generate maps of Upper Layer Heat content (ULH) for the Equatorial Atlantic. In order to validate the ULH estimates, we perform a comparison with an independent *in situ* data from Prediction and Research Moored Array in the Tropical Atlantic (PIRATA). There is a very good match between the ULH anomalies derived from remote sensing and from PIRATA moorings. The best correlations are for the northwest Equatorial Atlantic PIRATA buoys, while the worst correlations are for the southeastern Equatorial Atlantic sites. We believe that using the most recent World Ocean Atlas 2009 (WOA09), which already incorporates the PIRATA dataset, could further improve the present method.

Keywords: sea level anomalies, sea surface temperature, upper ocean heat content, altimetry, remote sensing.

RESUMO. Neste trabalho, nove anos (1998-2006) de dados de anomalias de elevação da superfície do mar, oriundos da integração de vários altímetros e distribuídos pela *Archiving Validation and Interpretation of Satellite Data in Oceanography* (AVISO), dados de temperatura da superfície do mar provenientes do sensor *TRMM Microwave Imager*, assim como dados climatológicos do *World Ocean Atlas 2001* (WOA01) são combinados através de um modelo de gravidade reduzida, assim como um modelo estatístico, para a geração de mapas do conteúdo de calor na camada superior do oceano para o Atlântico Equatorial. A fim de validar os dados de conteúdo de calor, realizamos uma comparação com dados independentes *in situ* do *Prediction and Research Moored Array in the Tropical Atlantic* (PIRATA). Há uma concordância muito boa entre as anomalias de calor na camada superior do oceano derivadas a partir dos dados de sensoriamento remoto e obtidas a partir das bóias do PIRATA. As melhores correlações ocorrem para as bóias localizadas no Atlântico Equatorial Noroeste, enquanto que as piores correlações ocorrem para as bóias localizadas no Atlântico Equatorial Sudeste. Acredita-se que a utilização do mais recente conjunto de dados do *World Ocean Atlas 2009* (WOA09), que incorpora os dados das bóias PIRATA, poderia melhorar ainda mais o presente método.

Palavras-chave: anomalias da elevação do nível do mar, temperatura na superfície do mar, conteúdo de calor na camada superior do oceano, altimetria, sensoriamento remoto.

[1]Universidade Federal do Rio de Janeiro, Instituto de Matemática, Departamento de Métodos Matemáticos, Av. Athos da Silveira Ramos s/n, C.T., Bl. C, Cidade Universitária, Ilha do Fundão, P.O. Box 68530, 21945-970 Rio de Janeiro, RJ, Brazil. Phone: (21) 2562-7508 ext. 222; Fax: (21) 2260-1884 – E-mail: wilton@ufrj.br

[2]Universidade Federal da Bahia, Instituto de Física, Departamento Física da Terra e do Meio Ambiente, Travessa Barão de Jeremoabo s/n, Campus Ondina, 40170-280 Salvador, BA, Brazil. Phone: (71) 3283-6683; Fax: (71) 3283-6681 – E-mail: clentini@ufba.br

[3]Tropical Oceanography Group (GOAT) – www.goat.fis.ufba.br

INTRODUCTION

One of the main goals of climate variability research is to predict relatively long-term changes in global climate. Due to the ocean's high thermal inertia it is believed that the Earth's climate is adjusted by the ocean's troposphere, where heat fluxes play a vital role on the air-sea interaction processes. Therefore, the amount of heat within the upper layer of the ocean is crucial to understand the coupling between the atmosphere and the ocean, and how they influence each other from short to long time scales.

The lack of continuous long-term hydrographic observations in some regions, specially in the South Atlantic Ocean, make satellite derived data one of the main sources to investigate time and spatial variability from coastal regions to basin scales. Altimeter data, which is not affected by cloud coverage as infrared derived data, provide extremely useful information on the vertical thermal and dynamical structure of the upper ocean when combined with climatological hydrographic through a diagnostic model (Goni et al., 1996; Garzoli & Goni, 2000; Lentini et al., 2006).

Current research and operational weather models rely on satellite based sea surface temperature (SST) measurements in combination with climatological data to infer the upper ocean's thermal structure and heat content. The Upper Layer Heat content (ULH) can be defined as the amount of heat stored in a layer which extends from the surface to a pre-defined isotherm located in the thermocline.

Assuming that the dynamics of the upper layer of the ocean can be reproduced by a reduced gravity model, Arruda et al. (2005) calculated the Upper Layer Heat content (ULH) and investigated the relative contribution of its annual cycle and its non-seasonal variability on key regions in the South Atlantic.

The objective of this work is to compare the ULH generated maps as in Arruda et al. (2005) with the ones derived directly from the Prediction and Research Moored Array in the Tropical Atlantic (PIRATA). This validation will allow the use of synthetic ULH data to study climate variability in the Tropical Atlantic with high spatial and temporal resolution.

DATASETS

Satellite Altimetry Data

In this work, we use weekly maps of Sea Level Anomalies (SLA) from multimission altimeter data products produced by Ssalto/Duacs and distributed by AVISO (Archiving Validation and Interpretation of Satellite Data in Oceanography) at www.aviso.oceanobs.com. The dataset spans from October 1992 to December 2006 with a 1/3-degree georeferenced on a Mercator grid.

Microwave Sea Surface Temperature Data

The Optimally Interpolated Sea Surface Temperature (SST) data are derived from the TRMM Microwave Imager (TMI) carried on NASA's Tropical Rainfall Measuring Mission (TRMM) satellite. This dataset provides daily images with a spatial resolution of 1/4-degree which goes from 1998 to 2006. This dataset is produced by Remote Sensing Systems and sponsored by National Oceanographic Partnership Program (NOPP), the NASA Earth Science Physical Oceanography Program, and the NASA MEaSUREs DISCOVER Project. Data are freely available, for research purpose, at www.remss.com.

Climatological Data

Climatological *in situ* temperature and salinity data are derived from the high resolution 1/4-degree World Ocean Atlas 2001 (WOA01) (Boyer et al., 2005). The World Ocean Atlas is a data product distributed by the Ocean Climate Laboratory of the National Oceanographic Data Center (NODC-U.S.) at www.nodc.noaa.gov/OC5/indprod.html.

Mooring Data

PIRATA is a multinational cooperation program designed to study ocean-atmosphere interactions in the Tropical Atlantic that affect regional climate variability on seasonal, interannual and longer time scales. The array was originally developed in the mid-1990s and has undergone expansions and enhancements since 2005 to improve utility for describing, understanding, and predicting societally relevant climate fluctuations. The PIRATA data can be freely downloaded from NOAA/PMEL website (www.pmel.noaa.gov/pirata).

All datasets are interpolated in space to the AVISO SLA grid, and the SST daily product is averaged weekly.

METHODS

We assume that the upper ocean dynamics can be reproduced by a reduced gravity model. In the equatorial region, the 20°C isotherm is approximately located in the middle of the thermocline (Merle, 1983) and it is highly correlated with sea level (Chaen & Wyrtki, 1981; Rebert et al., 1985). Consequently, we take it as the lower bound for the upper layer in the model. According to Goni et al. (1996), the altimetric SLA and climatological subsurface data can be combined in order to obtain an estimate of the horizontal and temporal variations of the depth of a chosen isotherm, which here is defined as the

depth of the 20°C isotherm (D_{20})

$$D_{20}(x, y, t) = \overline{D_{20}}(x, y) + \frac{g}{g'(x, y)}\eta(x, y, t), \quad (1)$$

where: $\overline{D_{20}}$ is the climatological 20°C isotherm depth (derived from WOA01 temperature data), g is the gravity, g' is the reduced gravity (calculated form climatological WOA01 temperature and salinity data), and η is the altimetric SLA.

In thermodynamics, the quantity of heat, ΔQ, gained by a body of fluid of unit volume and density ρ_0, when temperature is raised from T_0 to T (in °C) is $\Delta Q = \rho_0 c_p(T - T_0)$, where c_p is the specific heat at constant pressure. So, the amount of heat (divided by $\rho_0 c_p$) in a column of water that extends from the surface up to the depth of the 20°C isotherm (with a unit cross section area) is

$$\begin{aligned} ULH(x, y, t) &= \int_{D_{20}(x,y,t)}^{0} (T(x, y, z, t) - 20)\, dz \\ &= (ULT(x, y, t) - 20)\, D_{20}(x, y, t), \end{aligned} \quad (2)$$

where: T is temperature (°C) and the Upper Layer Temperature (ULT) is the mean temperature in the layer bounded below by the 20°C isotherm. In other words,

$$\begin{aligned} &ULT(x, y, t) \\ &= \frac{1}{D_{20}(x, y, t)} \int_{D_{20}(x,y,t)}^{0} T(x, y, z, t)\, dz. \end{aligned} \quad (3)$$

Since subsurface temperature measurements with high space and time coverage are not available, the integral in Equation (3) is calculated through the following equation,

$$ULT(x, y, t) = \alpha_0(x, y) SST(x, y, t) + \alpha_1(x, y, t), \quad (4)$$

where: $\alpha_0(x, y)$ and $\alpha_1(x, y)$ are the regression coefficients obtained when a linear regression is applied to all climatological values of (SST, ULT) from WOA01 in a $4° \times 4°$ box centered at (x, y), and $SST(x, y, t)$ is the sea surface temperature measured by the TMI sensor.

Therefore, the Upper Layer Heat content (ULH) is calculated according to the following expression,

$$\begin{aligned} ULH(x, y, t) = &\big(\alpha_0(x, y) SST(x, y, t) \\ &+ \alpha_1(x, y, t) - 20\big) D_{20}(x, y, t). \end{aligned} \quad (5)$$

Most of the previous estimates of Upper Ocean Heat Content from altimetry were based on the method proposed by Chambers et al. (1997). In that paper, the authors assumed that changes in the heat content could be related to changes in sea level by a linear relationship based on the assumption that the upper layer expansion/contraction was mainly due to temperature variations. Since changes in salinity could also affect the sea level, very few works (e.g., Polito et al., 2000; Sato et al., 2000) tried to estimate the haline correction for the sea level anomaly from hydrographic data prior the application of Chambers' method. Moreover, their method implicitly assumes that heat is integrated from a fixed depth up to the sea surface. Differently, our method uses a regional reduced gravity model to infer variations in the thermocline depth (Eq. (2)), and the estimated heat content is obtained by vertically integrating the temperature variations in a layer of non uniform thickness (Eq. (5)).

Using Equation (5), maps of ULH with the same spatial and temporal resolution of the altimetry data from 1992 to 2006 were generated. We illustrate the outputs of the described method by plotting in Figure 1, maps of average ULH and SST for the wet and dry seasons in the northwestern Brazil. We can see (Fig. 1a) that during the wet season, an area of high ULH (>750°C m) is formed off coast of NE Brazil between 5°S and 20°S. During the dry season, that area of high ULH diminishes and concentrates around 10°S. Also, north of the Equator, in the region of North Brazil Current retroflection (between 0°N and 10°N), an area of high ULH is formed. In the North Atlantic, we can identify part of the region of high ULH defined by Wang et al. (2006) as Atlantic Warm Pool. Comparing the left and right hand plots in Figure 1, we can observe that the ULH maps are not mirror images of the SST maps, so they bring additional information that is valuable for climate studies.

In order to assure the liability of this satellite derived dataset for climatic study purposes, a comparison between *in situ* data calculated from the Pilot Research Moored Array in the Tropical Atlantic (PIRATA) was performed. The PIRATA mooring sites were selected for comparison according to their maximum extent of available data and minimum gaps of missing values, which, when seen, were interpolated prior to the analysis. The selected locations are displayed on Figure 2.

RESULTS AND DISCUSSION

Figures 3 to 7 show the comparison between the satellite derived properties (thick line) and the *in situ* data (thin line) at five different PIRATA mooring sites. Care should be taken when analyzing each of these figures as the lengths of the five time series are not always coincident due to the availability of PIRATA data. The satellite derived depth of the 20°C isotherm (D_{20}, top

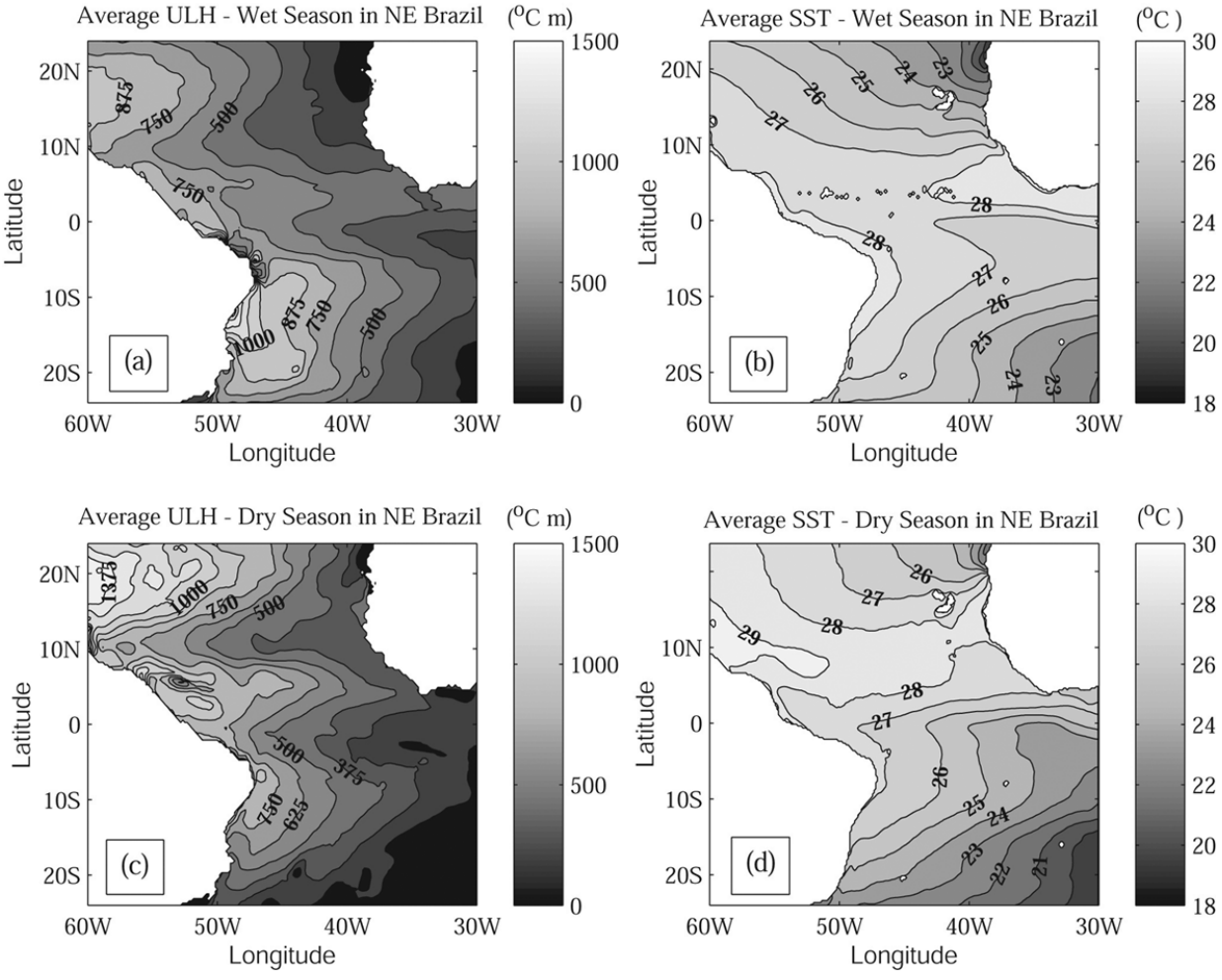

Figure 1 – (a) Average ULH (°C m) for the wet season (from November of one year to July of the following year) in NE Brazil; (b) Average SST (°C) for the wet season in NE Brazil; (c) Average ULH (°C m) for the dry season (August, September and October) in NE Brazil; (d) Average SST (°C) for the dry season in NE Brazil.

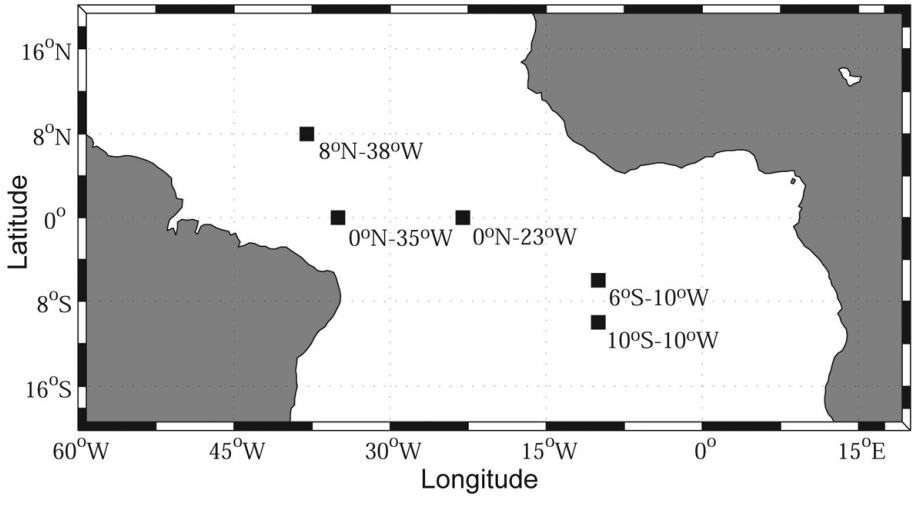

Figure 2 – Schematic representation of the PIRATA buoy locations used here for comparison between *in situ* data and satellite derived data.

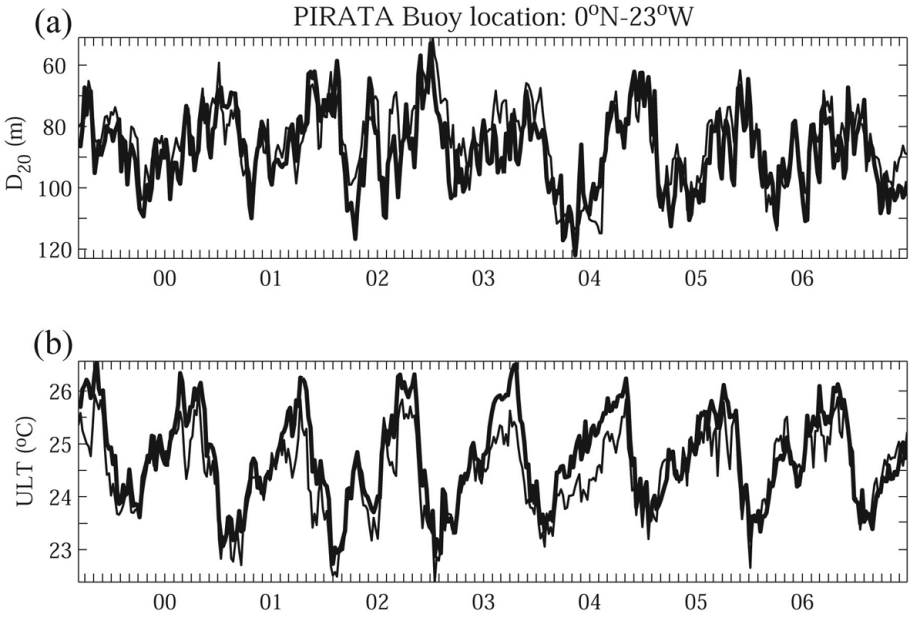

Figure 3 – Time series of (a) the depth of the 20°C isotherm (D_{20}, in meters) and (b) the average ULT (°C) estimated from satellite data (thick line) and derived from the PIRATA *in situ* data (thin line) at 0°N-23°W.

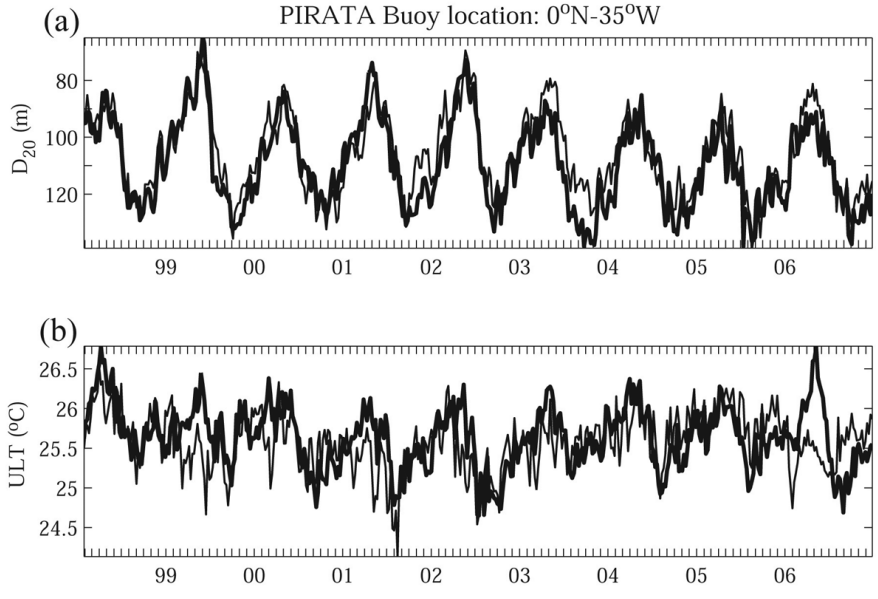

Figure 4 – Same as Figure 2, but for PIRATA buoy at 0°N-35°W.

panel) is computed through Equation (1), whereas the ULT (°C, bottom panel) is obtained from Equation (4). For the location of each PIRATA buoy, the reader should refer to Figure 2.

The two equatorial buoys located at 0°N-23°W and 0°N-35°W show an excellent agreement between the satellite derived D_{20} and ULT, and the *in situ* derived data obtained directly from the PIRATA buoys for the period of Jan-1999 to Dec-2006 (Fig. 3) and Jan-1998 to Dec-2006 (Fig. 4). However, one can notice that the satellite based ULT has a tendency for warmer temperatures, which can reach up to 0.7°C in some years, as it is the case for 2003 and 2004 (Fig. 3, bottom panel).

On the other hand, for the two buoys located at 6°S-10°W and 10°S-10°W in the southeastern Equatorial Atlantic the D_{20} is deeper than observations (e.g., $\approx$ 20 meters) specially during

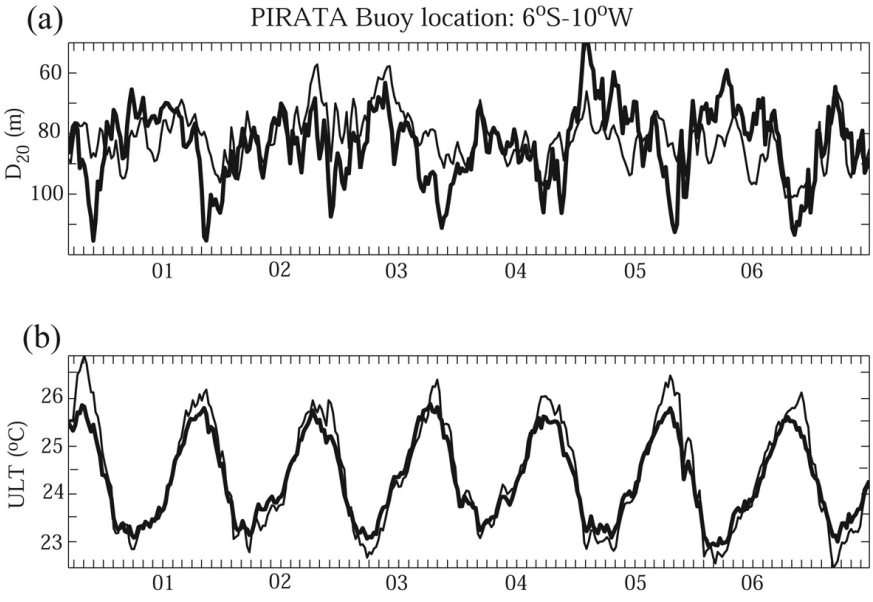

Figure 5 – Same as Figure 2, but for PIRATA buoy at 6°S-10°W.

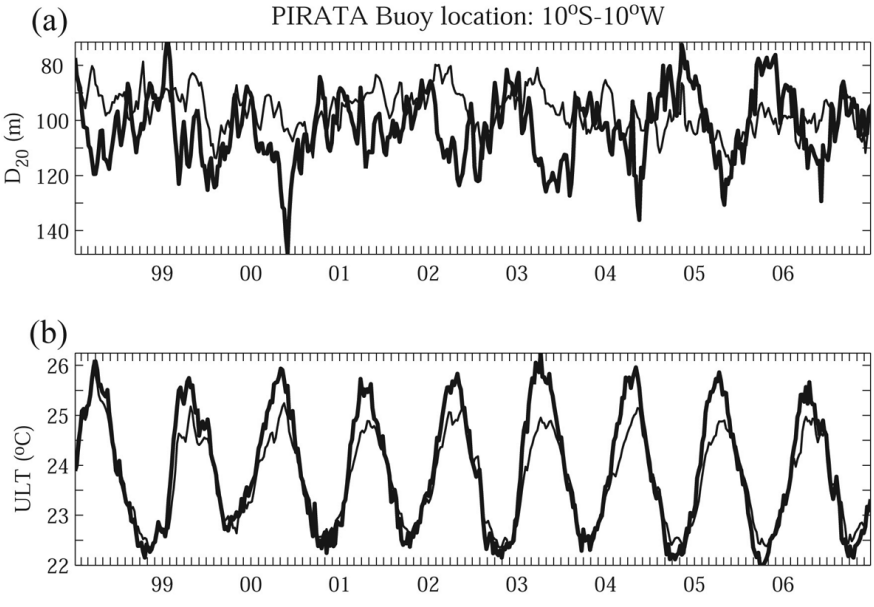

Figure 6 – Same as Figure 2, but for PIRATA buoy at 10°S-10°W.

the first semester of each year until 2003 (Figs. 5 and 6). From 2004 on, the satellite derived D_{20} is shallower than the observed for the next three years. The ULT shows an opposite pattern for these two locations. The satellite based ULT seems to be underestimated when compared to the PIRATA *in situ* observations at the mooring site located at 6°S-10°W (Fig. 5, bottom panel, thick line) for the whole period (i.e., Jan-2000 to Dec-2006). The ULT for the 10°S-10°W buoy, on the other hand, shows an opposite behavior, where the satellite derived data always seem to overestimate the peak of highest temperature, reaching up to a difference of ~1.0°C in 2003 when compared to PIRATA observations (Fig. 6, bottom panel, thick line). At this same location, the estimated ULT is higher than the observed during summer months (Fig. 6, bottom panel, thick line).

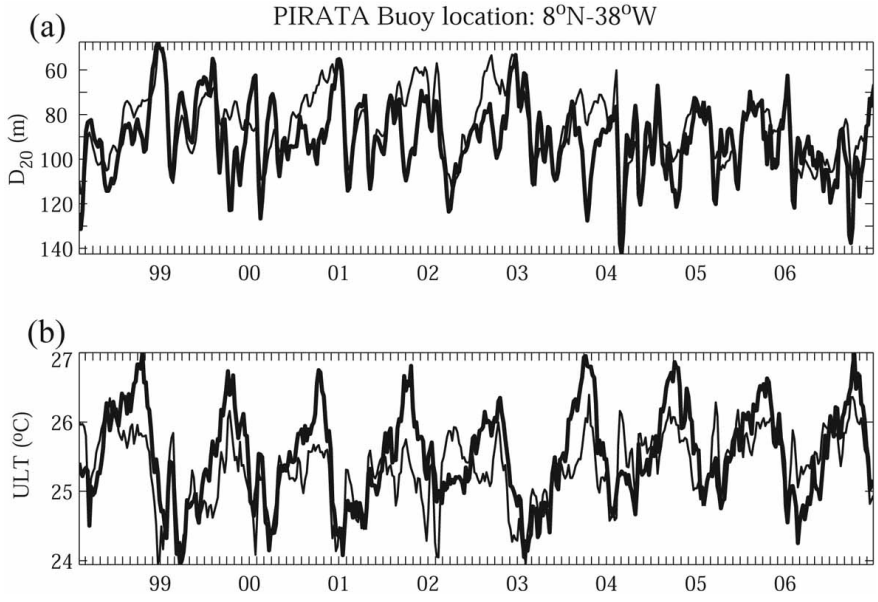

Figure 7 – Same as Figure 2, but for PIRATA buoy at 8°N-38°W.

The satellite derived D_{20}, computed for the northern hemisphere mooring site located at 8°N-38°W (Fig. 7), seems to match quite well to the observations, although it shows a tendency for increasing the depth of 20°C isotherm (e.g., $\approx$ 20 meters) specially during the second semester of each year until 2003. From 2004 on, this tendency disappears and now the behavior of computed D_{20} follows pretty much the behavior of the observed data. Analogous to what was described for the buoy at 10°S-10°W, the estimated ULT derived from Equation (4) is usually higher all year long with a slight tendency for warmer temperatures during the second semester of each year (Fig. 7). One can observe that both, D_{20} and ULT derived from remote sensing, have annual cycles with higher amplitudes than the observed ones.

If one looks carefully at the behavior of the time series shown on Figures 3 to 7, it is clear that the match between PIRATA *in situ* and satellite derived data improved quite significantly after 2003, specially, for the equatorial buoys. Although, some errors could be introduced when computing the *in situ* derived properties due to the fact that the PIRATA temperature sensors are depth-fixed to the ATLAS moorings (i.e., the depth of the 20°C may not be well represented by these sensors fixed depths), there are other important issues brought up by the scientific community lately that could potentially influence such errors. One of them is the global climatic change. The Intergovernmental Panel on Climate Change (IPCC) estimated, for the decade 1993-2003, a rise in the mean sea level, half of which is explained by the warming of the water and the remainder being essentially due to shrinking glaciers and polar ice caps (IPCC, 2007). However, since 2003 thermal expansion seems to have stopped growing, while the mean level of the ocean continues to rise, albeit at a slower rate. This piece of evidence could explain the significant observed improvement seen in the satellite derived data from 2004 on. Another important issue is the variability introduced by phenomena as the El Niño-Southern Oscillation (ENSO) and North Atlantic Oscillation (NAO). These events affect the dynamics as well as the thermodynamic balance in the region of study.

In order to find the reason why remote sensing ULT estimates differ from *in situ* observations, we carefully looked at the linear regressions between ULT and SST used in Equation (4). Figure 8 displays the scatter plot of SST *vs.* ULT from PIRATA data: (i) 0°N-23°W and (ii) 0°N-35°W at the Equator, (iii) 10°S-10°W in the southeastern Equatorial Atlantic, and (iv) 8°N-38°W in the northwestern Equatorial corner. The straight lines show the linear regression between SST and ULT from PIRATA data (solid lines), and between SST and WOA01 data (dashed lines) at four mooring sites in $4^\circ \times 4^\circ$ boxes centered at each buoy location. Note that the linear regression for *in situ* PIRATA data is for a fixed point in space (buoy location) using all available data for that point in time, while the linear regression for the climatological data is for all available points in space located in a $4^\circ \times 4^\circ$ box centered at an specific buoy location.

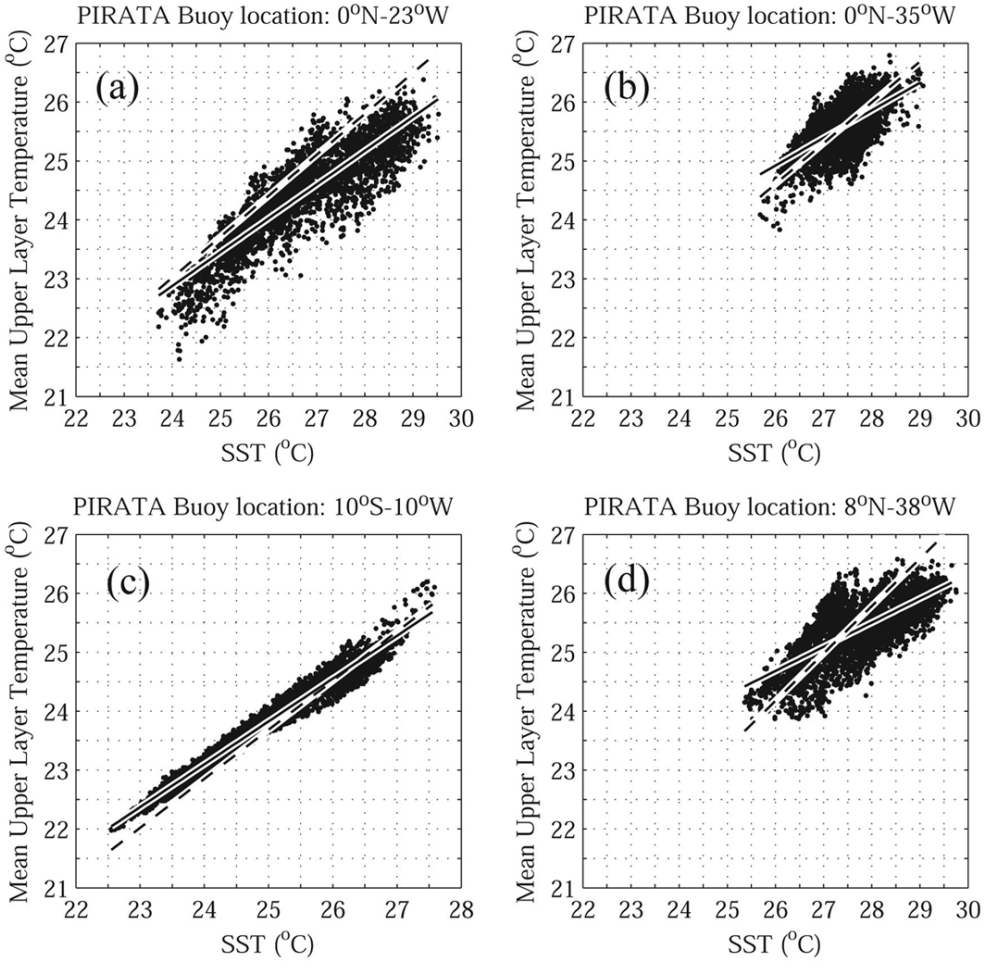

Figure 8 – Scatter plots of SST (°C) against mean ULT (°C) from PIRATA *in situ* data at the following mooring locations: (a) 0°N-23°W; (b) 0°N-35°W; (c) 10°S-10°W and (d) 8°N-38°W. Solid lines show the linear regression fit calculated from the PIRATA data at each location, whereas the dashed lines are the linear fit calculated from the WOA01 data in 4°×4° boxes centered at each PIRATA buoy location.

At 0°N-23°W there is a very good linear relationship between SST and ULT with a coefficient of determination r^2 of 0.87 (Fig. 8a). Note that the regression line derived from WOA01 (dashed line) is above the one derived from PIRATA data at that location. This means that Equation (4) has a tendency to always overestimate ULT for high SSTs, what causes the high observed values for estimated ULT during austral summer months (Fig. 3).

The buoy located at 0°N-35°W shows a cloud of scattered points which concentrates around the values of 27.5°C for SST and 25.5°C for ULT (Fig. 8b). The correlation between SST and ULT is r^2 = 0.60, which makes the error introduced by using the regression line derived from WOA01 (dashed line) smaller. For high (low) SST (>28°C), the calculated ULT from Equation (4) tends to be overestimated (underestimated), which tends to take place during austral summer (winter) mainly.

At 10°S-10°W there is a high linear relationship between SST and ULT with a r^2 of 0.99 (Fig. 8c). The ULT computed from Equation (4) tends to be overestimated during austral summer and underestimated during austral winter when the linear regression coefficients derived from WOA01 climatology are used (Fig. 6).

The regression between SST and ULT at 8°N-38°W (Fig. 8d) has a r^2 of 0.7. Since the data are more scattered, the ULT computed from Equation (4) tends to be also significantly overestimated (underestimated) during austral summer (winter) (Fig. 7).

The comparisons between *in situ* derived and satellite derived upper layer heat content (ULH) computed at each PIRATA buoy locations (see Fig. 2) are shown on Figures 9 to 13 (solid lines). The dashed lines represent the seasonal fit to the ULH time series as a combination of annual and semiannual harmo-

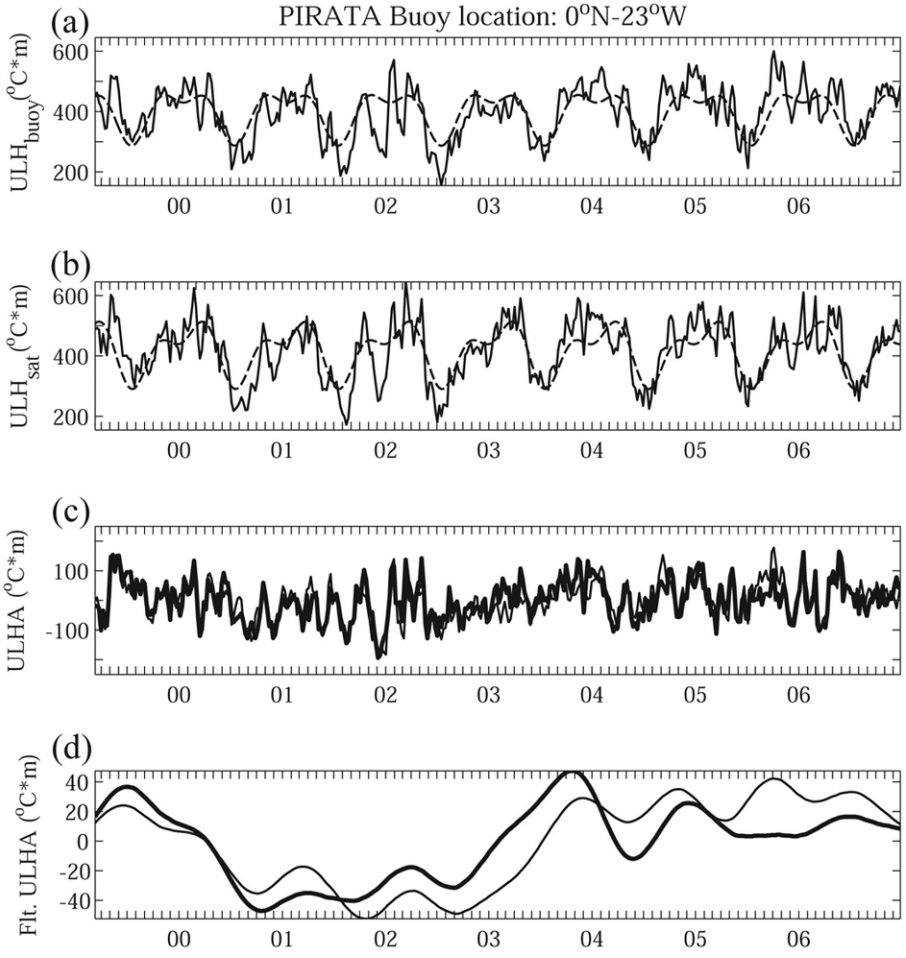

Figure 9 – Time series of ULH (°C m) for the PIRATA buoy location at 0°N-23°W derived from (a) observations and (b) satellite (solid line), and their associated fitted seasonal cycle (annual plus semiannual harmonics, dashed line), respectively. Comparison between the time series of (c) the PIRATA *in situ* based (thin line) and satellite derived (thick line) ULHAs (°C m), and (d) same as (c) but low-pass filtered with cut off period of 12 months. The anomaly time series is computed as the difference between the original ULH time series and its seasonal fit.

nics, similarly to what was done to SSTs along the southeastern South American coastline in Lentini et al. (2000, 2001). For details of the method the reader should refer to Lentini et al. (2000).

For the two PIRATA mooring sites located at the Equator, both satellite derived ULH (Fig. 9b, solid line) and *in situ* derived ULH (Fig. 9a, solid line) are in good agreement, although the satellite based values always seem to slightly overestimate the peaks of maxima. On the other hand, the amplitude of the ULH and its respective seasonal cycle (Fig. 9b, dashed line) matches quite well the *in situ* ULH (Fig. 9a, dashed line), reaching values between 500-700°C m.

The southeastern Equatorial Atlantic buoys, 6°S-10°W and 10°S-10°W (Figs. 11 and 12), do not show the same behavior described above for the two equatorial PIRATA buoys. For example, the ULH computed from both observational and remote sensed data for the 6°S-10°W buoy have the same order of magnitude and show a similar sinusoidal behavior, where their ridges and troughs have almost the same amplitude. The same can be seen for their seasonal fits (Figs. 11a and b). On the other hand, the satellite derived ULH and the amplitude of its seasonal cycle for the 10°S-10°W mooring (Fig. 12b) is about twice as big as its observational counterpart and its associated seasonal fit (Fig. 12a). This is believed to be due to accumulated errors in the calculation of D_{20} and ULT at that location (Fig. 6).

The off-equatorial buoy located at the northwest Equatorial Atlantic corner (i.e., 8°N-38°W), does not show this difference, although the ULH derived from the altimeter presents a

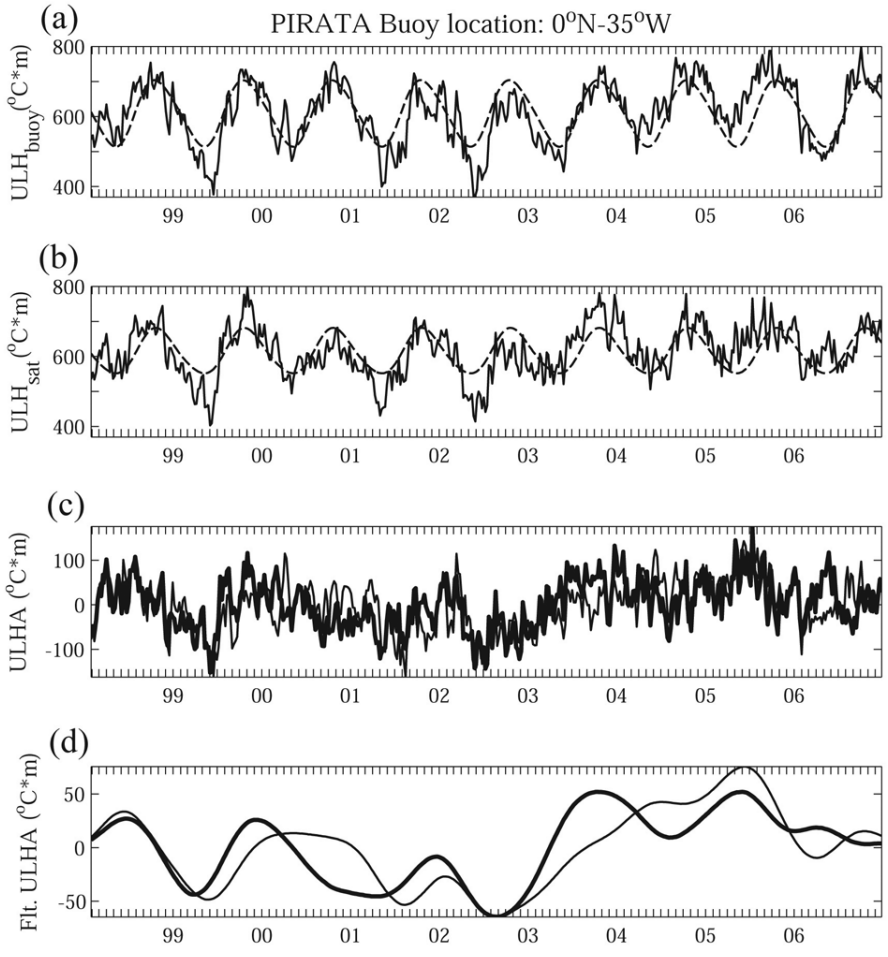

Figure 10 – Same as Figure 9, but for PIRATA buoy at 0°N-35°W.

more pronounced bias over the peaks of maxima (minima) in the time series having a tendency to overestimate (underestimate) the ULH values when compared to its observational counterpart (Fig. 13). Moreover, the contribution of the semiannual harmonic to the seasonal fit is clearly seen and is more evident than the one observed in the 0°N-23°W mooring.

Figures 9c to 13c show the Upper Layer Heat content Anomalies (ULHAs), which were computed as the difference between the ULH and its seasonal fit for satellite derived (thick line) and *in situ* based (thin line) estimates. It is remarkable that although some satellite estimates, as well as their seasonal fit, are quite different from some observational estimates, all the five selected PIRATA mooring sites show a correlation coefficient ≥ 0.54 for the unfiltered ULH (Table 1). The highest correlations are observed in the northwestern and western Equatorial Atlantic sections (i.e., 0.83 for the 8°N-38°W and 0.77 for the 0°N-35°W) respectively.

Another important issue is that the ULHAs show a positive trend (i.e., warming) from mid-2002 until mid-2004, except for the southeastern-most PIRATA buoy (see Fig. 2), which shows a random pattern around the zero line for this same period (Fig. 12c). This "warming" period needs further investigation, although we can observe that in these periods two ENSO events happened: a strong 2002-2003 El Niño, and a weak 2004-2005 El Niño.

The 10°S-10°W buoy presents a quite significant difference between the amplitude of the fitted seasonal cycle of the estimated ULH and *in situ* derived values, although the ULHAs fall into the same amplitude range and show a very close variability, with a correlation coefficient of 0.64 for the unfiltered data (Table 1).

Figures 9d to 13d show the low-pass filtered ULHAs (with cut off period of 10 months) for satellite based (thick line) and *in situ* derived (thin line) estimates. As previously discussed, the filtered time series of ULHAs in the PIRATA array located in the northwestern and western Equatorial Atlantic sections are

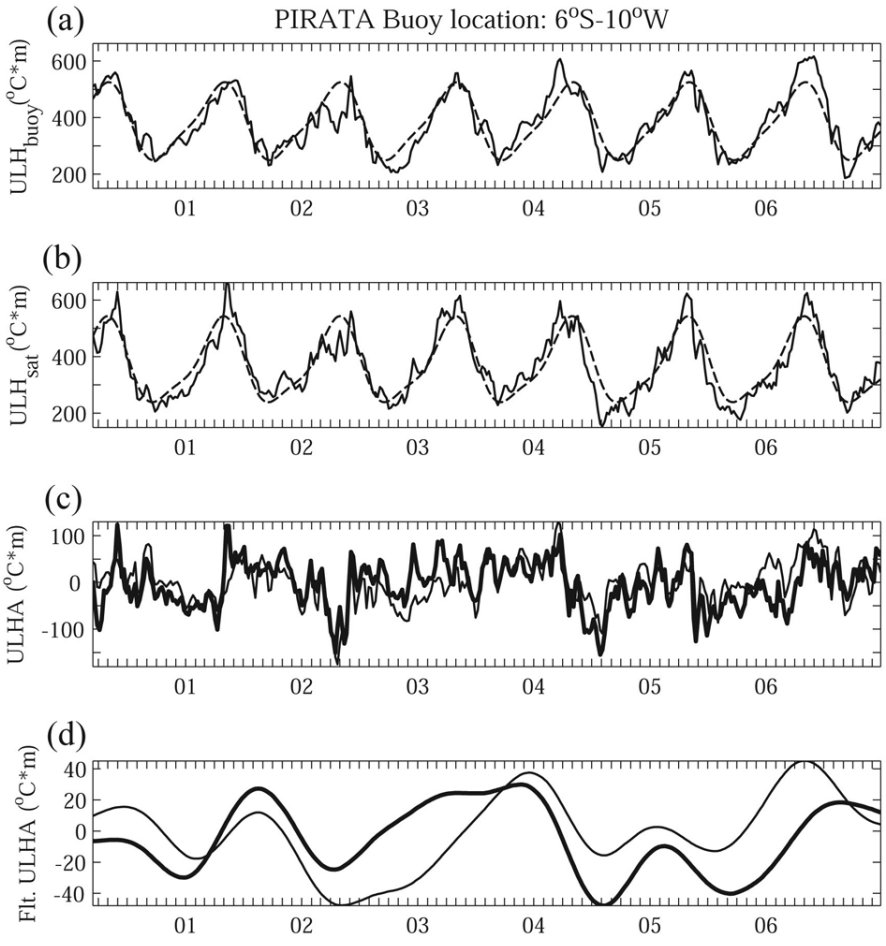

Figure 11 – Same as Figure 9, but for PIRATA buoy at 6°S-10°W.

highly correlated (i.e., $\geq$ 0.76), except for the two buoys moored at 6°S-10°W and 10°S-10°W, where the correlation coefficient drops down to 0.29 and 0.37, respectively (Table 1). These two low correlations are probably due to the errors introduced into the derived estimates when the WOA01 derived linear regression coefficients were applied to Equations (4) and (5), specially to the buoy located at 10°S-10°W.

Table 1 – Correlation between the time series of raw and filtered *in situ* based and satellite derived ULHAs (°C m) shown in Figures 8 to 12 panels (c) and (d), respectively.

Buoy location	Raw ULH correlation	Filtered ULH correlation
0°N-23°W	0.61	0.76
0°N-35°W	0.77	0.78
6°S-10°W	0.54	0.29
10°S-10°W	0.64	0.37
8°N-38°W	0.83	0.88

CONCLUSIONS

In this paper we compare the Upper Layer Heat Content data derived from remote sensing and *in situ* data collected from buoys of the PIRATA project. It is shown that the best correlation between calculated and *in situ* derived ULH anomalies is for the northwestern Equatorial Atlantic buoy, while the worst correlations are for the southeastern Equatorial ones. These results are expected since the North Atlantic is one of the best sampled regions in the World Oceans, while the South Atlantic is still one of the poorest ones.

As pointed out in the previous section, there is a significant improvement between *in situ* based and satellite derived data after 2003, which, according to the IPCC report (IPCC, 2007), is due to the stop-growing thermal expansion of mean sea level since this year. Although this piece of evidence can explain the quite perfect match between PIRATA derived and satellite derived data from 2004 on, specially for the equatorial PIRATA

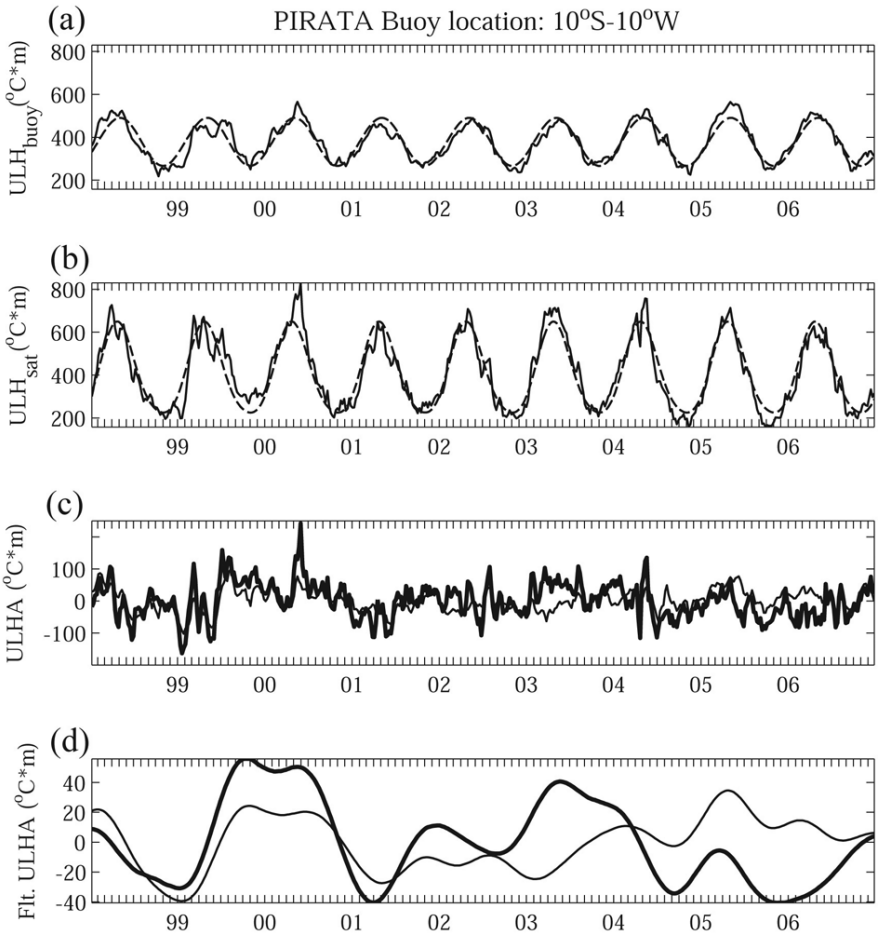

Figure 12 – Same as Figure 9, but for PIRATA buoy at 10°S-10°W.

moorings, some discrepancies still may be observed in the time series. These discrepancies could be caused by a number of factors: possible method limitations, the use of WOA01 data to estimate the regression coefficients in Equation (4), global climate change, and climatic variability phenomena like ENSO and NAO. It is believed that using the most recent World Ocean Atlas 2009 (WOA09) dataset, which already incorporates the PIRATA data, could further improve the method presented here. However, we decided not to use the WOA09 in order to make an independent comparison between our satellite based estimates and the PIRATA derived properties. Nevertheless, comparison among different measurement sources is needed in order to improve our understanding of upper ocean dynamics and their different associated climate variability scenarios.

Considering all approximations behind Equation (5), we conclude that the derived ULHA field is a valuable tool to study climate variability on the Equatorial Atlantic, due to the high spacial and temporal coverage of remote sensing data.

Therefore, it is clear that the ULH maps are potentially important to study the heat variability in the ocean, specially in the western Equatorial Atlantic where the upper limb of the Meridional Overturning Circulation Cell takes place. Another important aspect of its potential is the use of ULH maps as a proxy to monitor the development and occurrence of extreme events which may make landfall and increase abruptly the amount of precipitable water over coastal areas.

ACKNOWLEDGMENTS

The authors would like to thank The National Council for Scientific and Technological Development (CNPq-Brazil) for their financial support through the grant 478480/2009-1. This work is also part of the CATIN (*Clima do Atlântico Tropical e Impactos sobre o Nordeste*) project (CNPq grant 492690/2004-9). The authors are grateful for the suggestions and comments of the two anonymous referees that improved a lot the present work.

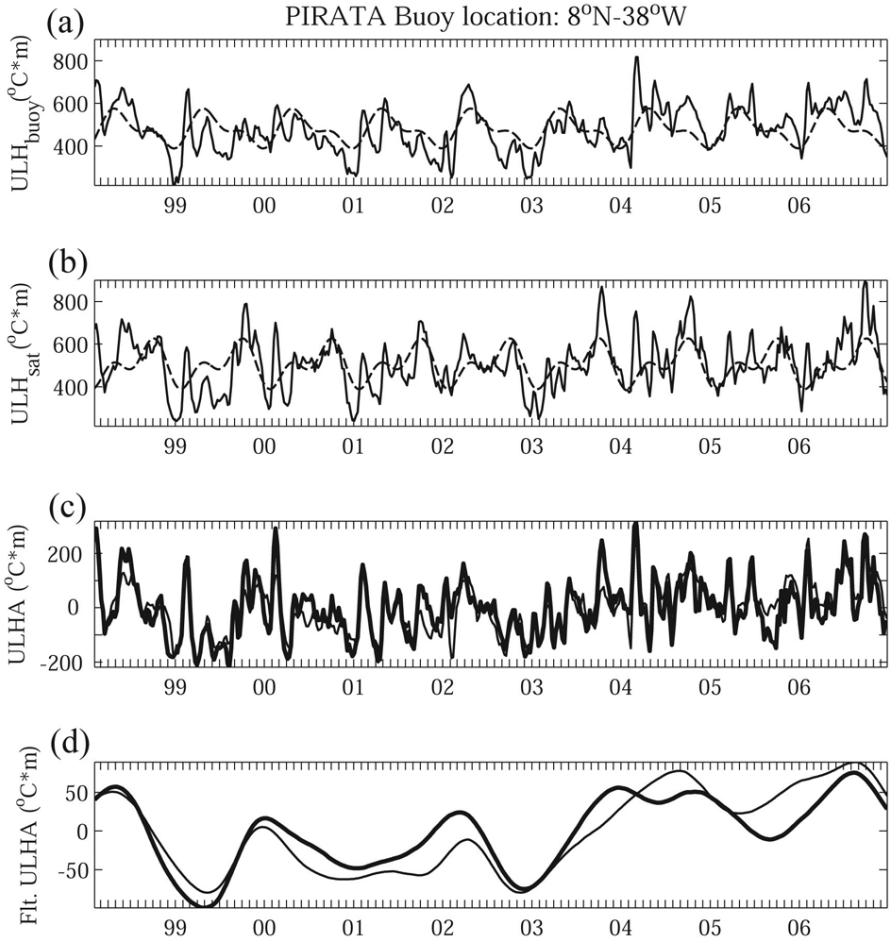

Figure 13 – Same as Figure 9, but for PIRATA buoy at 8°N-38°W.

REFERENCES

ARRUDA WZ, LENTINI CAD & CAMPOS EJD. 2005. The use of satellite derived upper layer heat content to study the climate variability in the South Atlantic. Rev. Bras. Cartogr. (Braz. J. Cartogr.), 57(2): 87–92.

BOYER T, LEVITUS S, GARCIA H, LOCARNINI RA, STEPHENS C & ANTONOV J. 2005. Objective analyzes of annual, seasonal, and monthly temperature and salinity for the world ocean on a 0.25 degrees grid. Int. J. Climatol., 25(7): 931–945.

CHAEN M & WYRTKI K. 1981. The 20°C isotherm depth and sea level in the western equatorial Pacific. J. Oceanogr. Soc. Jpn., 37: 198–200.

CHAMBERS DP, TAPLEY BD & STEWART RH. 1997. Long-period ocean heat storage rates and basin-scale heat fluxes from TOPEX. J. Geophys. Res., 102: 10525–10533.

GARZOLI S & GONI GJ. 2000. Combining altimeter observations and oceanographic data for ocean circulation and climate studies. In: HALPERN D (Ed.). Satellites Oceanography and Society. Elsevier Science, 79–97.

GONI GJ, KAMHOLZ S, GARZOLI S & OLSON DB. 1996. Dynamics of the Brazil-Malvinas Confluence based on inverted echo sounders and altimetry. J. Geophys. Res., 101: 16273–16289.

IPCC. 2007. Climate Change 2007: The Physical Science Basis. Contribution of Working Group I to the Fourth Assessment Report of the Intergovernmental Panel on Climate Change. In: SOLOMON S, QIN D, MANNING M, CHEN Z, MARQUIS M, AVERYT KB, TIGNOR M & MILLER HL (Eds.). Cambridge University Press, Cambridge, United Kingdom and New York, NY, USA, 996 pp.

LENTINI CAD, CAMPOS EJD & PODESTÁ GG. 2000. The annual cycle of satellite derived sea surface temperature on the Western South Atlantic shelf. Braz. J. Oceanogr., 48(2): 93–105.

LENTINI CAD, PODESTÁ GG, CAMPOS EJD & OLSON DB. 2001. Sea surface temperature anomalies in the Western South Atlantic from 1982 to 1994. Cont. Shelf Res., 21: 89–112.

LENTINI CAD, GONI GJ & OLSON DB. 2006. Investigation of Brazil Current Rings in the confluence region. J. Geophys. Res., 111, C06013, doi: 10.1029/2005JC002988.

MERLE J. 1983. Seasonal Variability of Subsurface Thermal Structure in the Tropical Atlantic Ocean. In: NIHOUL JCJ (Ed.). Hydrodynamics of the Equatorial Ocean. Proceedings of the 14th International Liege Colloquium on Ocean Hydrodynamics. Elsevier Oceanography Series, 36: 31–49.

POLITO PS, SATO OT & LIU WT. 2000. Characterization and validation of the heat storage variability from TOPEX/Poseidon at four oceanographic sites. J. Geophys. Res., 105(C7): 16911–16921.

REBERT JP, DONGUY JR & ELDIN G. 1985. Relations between sea level, thermocline depth, heat content, and dynamic height in the Tropical Pacific Ocean. J. Geophys. Res., 90(C6): 11719–11725.

SATO OT, POLITO PS & LIU WT. 2000. Importance of salinity measurements in the heat storage estimation from TOPEX/POSEIDON. Geophys. Res. Lett., 27(4): 549–551.

WANG C, ENFIELD DB, LEE SK & LANDSEA CW. 2006. Influences of the Atlantic Warm Pool on Western Hemisphere Summer Rainfall and Atlantic Hurricanes. J. Climate, 19(12): 3011–3028.

NOTES ABOUT THE AUTHORS

Wilton Zumpichiatti Arruda. Bachelor in Computer Science (UFRJ/1990), Master and Doctor in Mathematics (UFRJ/1991, 1996), and Ph.D. in Physical Oceanography at the Florida State University (2002). He teaches at the Institute of Mathematics of the Universidade Federal do Rio de Janeiro (UFRJ) since 1995, and he is an Associate Professor since 2009. His areas of interest are: upper ocean dynamics, ocean circulation, ocean modeling, climate variability, and satellite oceanography among others.

Carlos Alessandre Domingos Lentini. Ph.D. in Physical Oceanography and Meteorology at the Rosenstiel School of Marine and Atmospheric Science of the University of Miami (2002). He was a postdoc at the Oceanographic Institute of the Universidade de São Paulo (2002-2005), and at the Fundação Cearense de Meteorologia e Recursos Hídricos (2006). He holds an Adjunct faculty position at the Universidade Federal da Bahia (UFBA) since 2007. His areas of interest are: upper ocean dynamics, climate variability, oceanography from space, bio-physical interactions, and large and mesoscale dynamics with emphasis on the Southwest and Tropical Atlantic.